

ADJUSTING bERLinPro OPTICS TO COMMISSIONING NEEDS*

B. Kuske[†], M. McAteer, Helmholtz-Zentrum für Materialien und Energie, Berlin, Germany

Abstract

bERLinPro is an Energy Recovery Linac (ERL) project being set up at HZB, Berlin. During the turn of the project, many adaptations of the optics to changing hardware realities and new challenges were necessary. Exemplary topics are chosen for each of the three different machine parts: the diagnostics line, the Banana and the recirculator. In the diagnostics line, the need to seek a quick understanding of the machine during commissioning and the low energy are the central concern. In the Banana, unwanted beam will dominate the performance. Commissioning of the recirculator will be realized with the super-conducting linac module fabricated for the Mainz ERL project MESA, as the bERLinPro linac is delayed. The Mainz linac will supply 60% of the energy planned. While the adopted optics shows similar parameters as the original 50 MeV optics, studies of longitudinal space charge and coherent synchrotron radiation show that the lower energy leads to large emittance blow up due to micro bunching and CSR effects.

INTRODUCTION

bERLinPro is an Energy Recovery Linac project close to completion at HZB, Berlin, Germany, [1]. It is intended as an experiment in accelerator physics, to pioneer the production of high current, low emittance beams in a fully super-conducting accelerator, including SRF gun, booster and linac. The machine, with a length of roughly 80 m consists of three different independent sub-parts: the diagnostics line, straight forward from the SRF gun and booster; the low energy part, including injector, merger, linac straight, splitter and dump line. This is called the Banana. In presence of a linac module, the beam would run through the recirculator and be energy recovered before being led to the dump line, Fig. 1. Over the turn of the project different boundary conditions asked for optics adjustments and new challenges had to be met. The paper describes examples of this work for each machine part.

DIAGNOSTICS LINE

The diagnostics line consists of the 1.3 GHz, 1.4 cell, single cavity SRF gun, providing up to 3 MeV electrons with a design bunch charge of 77 pC. The gun module also hosts two corrector coils (H/V) and a cold solenoid. The booster, hosting three two-cell cavities can boost the energy up to 6.5 MeV. The first cavity imprints a chirp on the bunch for velocity bunching, while the other two cavities are run on crest for acceleration. Further elements are 6 quadrupoles, a transverse deflecting cavity, a spectrometer followed by a 300 W

* Work supported by German Bundesministerium für Bildung und Forschung, Land Berlin and grants of the Helmholtz Association
[†] bettina.kuske@helmholtz-berlin.de

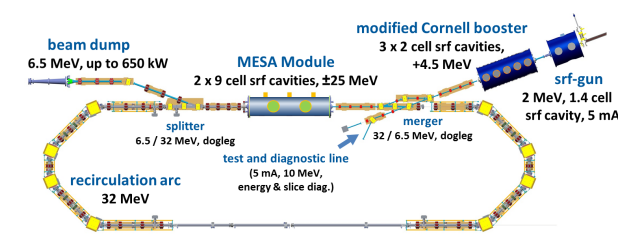


Figure 1: Layout of bERLinPro with the diagnostics line in straight continuation of the gun, the low energy part (Banana) from gun to dump, and the recirculator with the MESA module.

Faraday cup, or, straight ahead, a 35 kW beam dump, Fig. 2. Optics were developed including the booster (6.5 MeV) and with three booster replacement quadrupoles (taken from the recirculator) and 2.7 MeV. Four beam position monitors (BPM) and two screens (FOM) are available for diagnostics. Two laser systems are available: a 50 MHz laser providing single bunches at frequencies between 1 Hz and 100 kHz, corresponding to 77 pA to 8 μA, or up to 4 mA cw; and a 1.3 GHz laser providing macro pulses from 1 Hz to 1 kHz, 6 nA to 20 μA, or up to 100 mA cw.

As any linear accelerator, an ERL is an initial value problem: without exact knowledge of the initial parameters of the beam, a later understanding and characterization of the beam parameters is difficult. Therefore, a thorough understanding of the gun is indispensable. The gun enables the low emittance and the stability of the complete machine due to the laser- and RF stability and the synchronization between the two. Most of the unwanted beam, from laser effects to field emission at 30 MV/m will originate in the gun and the machine up time is determined by the cathode life time. Finally, the goal of producing 100 mA is achieved in the gun (although with a second version, utilizing high power couplers).

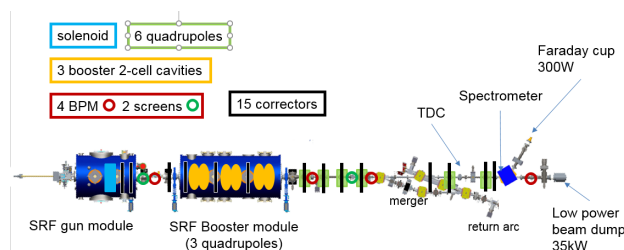


Figure 2: Diagnostics line: Intended for the characterization of gun and booster and initial beam parameters.

Before the gun is assembled and tested, many ambiguities arise, starting from the actual energy of the beam, over the bunch parameters, to the system parameters leading to successful acceleration. It is intended to use machine learning

Content from this work may be used under the terms of the CC BY 3.0 licence (© 2019). Any distribution of this work must maintain attribution to the author(s), title of the work, publisher, and DOI

or statistical learning to ease commissioning, see [2]. In addition, the number of independent parameters necessary to thread the beam successfully through the diagnostics line, should be minimized. Using the samples (tracking results of the diagnostics line for different machine parameters) produced for the machine learning attempts, dependencies can be identified via 'data mining'. Fig. 3 shows the example of the solenoid field setting, that leads to a comparable beam transport through the diagnostics line (black dots). It can be derived from the maximal gun field on axis and the cathode position (yellow surface). Here, cathode position '0' refers to no cathode retraction and position '6' means a recess of 2.5 mm.

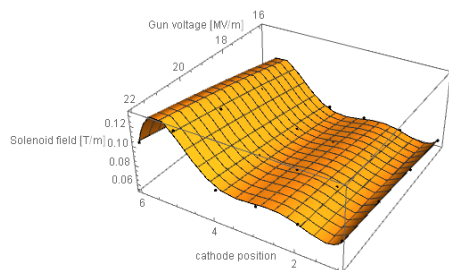


Figure 3: The solenoid field adequate to transport the beam through the beam line can be expressed as a function of cathode position and gun field.

Another option is to define the quadrupole settings, as to produce round beams on the screens for easier detection. For low currents, where the bunch is not space charge dominated, the set values can be simply scaled with energy.

Low energy beam

Analytic estimations of the influence of the earth magnetic field on the low energy beam from the gun indicate, that the trajectory might be influenced by external magnetic fields. Therefore, the magnetic field has been measured prior to the installation of magnets and girders in the subterranean hall. A 3D Hall-probe, installed on a small wagon at beam height, was moved along the future path of the electrons. The result is shown in Fig. 4. The strong, and strongly varying, vertical field (blue dots) of up to ± 1 G is caused by the reinforcement iron in floor and ceiling of the hall. The total height of the hall is only 3 m and the beam height is 1.2 m. Due to the larger distance from the side walls of the hall, the horizontal field is relatively stable between 0.2 G and 0.4 G. The step function indicates the realization of the field in the tracking code OPAL, [3]. After the installation of the girders and the lower half of the magnets, strong local magnetization was observed, partly due to remanent fields in the half-magnets, but also in the iron girders. After the completion of the installation and cycling of the magnets a third measurement will be carried out.

When the measured magnetic field was included in tracking studies, the beam got lost at the vacuum aperture 7 m behind the cathode. For comparison, no particle loss was detected during extensive error studies performed for the

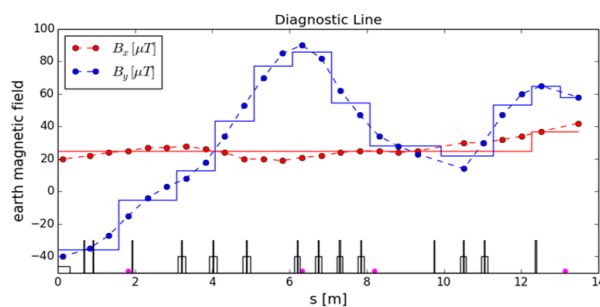


Figure 4: The magnetic field measured along the electron path in the diagnostics line, prior to the installation of magnets and girders.

complete machine, [4], [5]. Trajectory corrections using singular value decomposition of the response matrix revealed, that although more than sufficient corrector magnets are installed (except for inside the booster), we run short of BPMs in the diagnostic line, as well as in the Banana. As a consequence of these investigations, corrector coils are now also included in the booster module. Residual trajectory offsets of up to 7 mm in the horizontal plane remain after correction. Workarounds including beam based alignment, or the usage of calibrated response matrices, including the optics as well as the magnetic fields, have to be used to establish better corrections.

BANANA

In the low energy section of the machine, the 'Banana', the beam, after acceleration in the booster, passes through the merger chicane, through the straight section with three quadrupoles replacing the linac, and is then deflected into the dump line to the 650 kW beam dump, see Fig. 5. A single collimator is located in the merger at highest dispersion. In the Banana, the merger optics, the emittance compensation scheme, and the bunch compression will be verified. Halo studies can be performed.

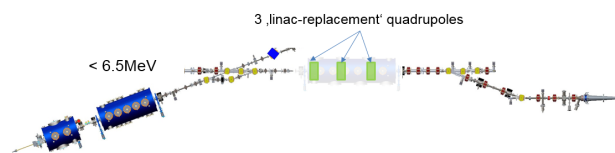


Figure 5: The layout of the low energy part of the machine (without linac).

It is expected that, for the operation of high current ERLs, the limit for beam halo at the entrance to the linac is in the order of 10^{-7} to 10^{-8} . A thorough understanding of sources of unwanted beam is therefore indispensable, so intense studies of 'unwanted beam' have been performed for the injector [6].

There are two major sources of unwanted beam: field emission from cavity and cathode surfaces, and laser-related effects. The magnitude of each source is installation-

dependent and only quantifiable after the start of operation. Predictions of possible transport of unwanted beam are based on Astra tracking studies.

Laser-related effects

The longitudinal tails of the laser pulse, transverse tails due to diffraction at the window where the laser pulse enters the cryomodule, and stray light that scatters off of imperfections in mirrors in the laser transport system all generate unwanted beam. Much of the beam from the longitudinal tails of the laser pulse can be collimated in the merger. The beam from transverse tails of the laser pulse will mostly pass through the merger and contribute to beam halo. About 20% of the electrons from stray light on the cathode (modeled as a uniform distribution in space and time of photons hitting the cathode) will have the correct energy to pass through the merger, and so will contribute to beam halo in the Banana or linac.

In addition, when operating in single-bunch or pulsed mode, there will be "ghost bunches" (low-charge electron bunches from incompletely-blocked laser pulses) between the full-charge electron bunches. The design extinction ratio for blocked laser pulses is 10^{-8} , but achieving that level of extinction is challenging and higher extinction ratio in the real machine is possible. These bunches will have different beam dynamics from full-charge bunches due to the reduced space charge effects. They will be critical in diagnostic mode, especially when the single-bunch rep rate is low, where they might spoil bunch measurements.

Field emission

The effects of "dark current" from field emission were studied in Astra tracking simulations. The simulations assumed a uniform distribution of emitters on the surface of the gun and booster cavities, on the cathode surface, and around the edge of the cathode plug.

Of the field emission electrons from the cathode and plug, most are lost on the aperture in the injector and merger. 5-10% of emitted electrons travel back to strike the cathode surface, which may reduce cathode lifetime. Several percent pass through the merger.

Of the electrons emitted from the gun cavity surface, the vast majority is lost within the cavity. A few percent strike the cathode surface, and a very small amount (around one permil) passes through the merger.

Of the electrons emitted from the booster surface, the vast majority is lost within the cavities or within the booster cryomodule. A very small amount (a couple permil) travels upstream to strike the cathode. Electrons that escape the cryomodule travelling downstream are lost in the merger.

RECIRCULATOR

The bERLinPro recirculator consists of two 180° arcs with four 45° rectangular dipoles each. The two central dipoles and the central quadrupole in each arc are moveable to enable path length adaptations. Two dipole chicanes, merger

and splitter, compensate for the kick necessary to deflect the low energy beam onto the linac axes and into the dump. The linac straight has a free length of 5.8 m.

The bERLinPro linac, Fig. 6, is planned with three five-cell cavities and elaborate wave guide HOM absorbers for high currents. It can boost the energy to 50 MeV. Due to the prioritization of a competing project at HZB, BESSY-VSR, the production of the linac had to be postponed.

The ERL project MESA, at the Mainz University, has the opposite problem: the linac module is delivered, but the civil construction plans had to be altered, and no building will be available to host the machine before 2022. A collaboration between the two projects has been established, that consists of testing the MESA module with beam at bERLinPro, [7]. The MESA module, Fig. 7, hosts two nine-cell Tesla-type

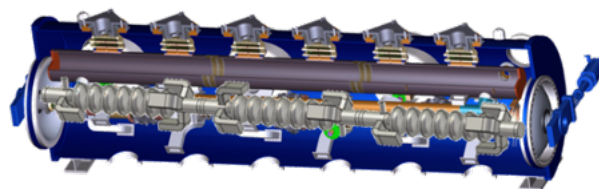


Figure 6: The layout of the bERLinPro linac module with elaborate wave guide HOM absorbers.

cavities. It is shorter than the bERLinPro module and capable to boost the energy to 30 MeV. The MESA project suffices with low currents so the HOM dampers consist of a notch-filter and a coupling antenna. HOMs will probably limit the current when running the module in bERLinPro to a few mA. The changes necessary in bERLinPro to host

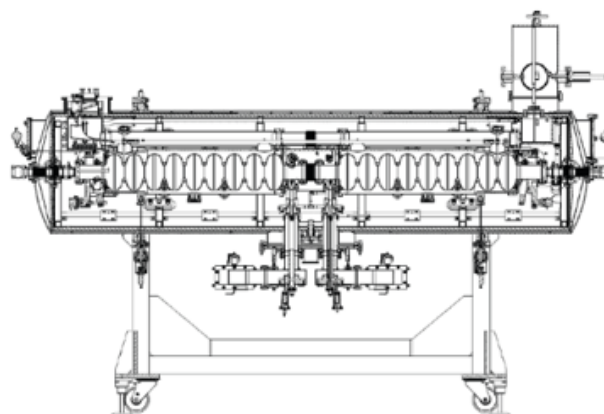


Figure 7: The layout of the MESA linac module with two Tesla-type cavities.

the MESA linac module have been described in detail in [7]. Geometrical differences were the different length and beam height. Technical differences like the He-supply from the side, as opposed to the top (MESA), or the cooling with

Content from this work may be used under the terms of the CC BY 3.0 licence (© 2019). Any distribution of this work must maintain attribution to the author(s), title of the work, publisher, and DOI

liquid nitrogen, not foreseen for bERLinPro, are manageable. The path length changes by 7.7 mm due to the lower energy, lies just within the range of the path length adaption of bERLinPro. The larger beam offset in the merger and splitter chicane of 55 mm lies well within the aperture of 80 mm. Two effects have to be accounted for, when adjusting the optics to the lower energy: the reduced RF focusing of the MESA linac due to the lower peak field of 23 MV/m on axis (compared to 35 MV/m) and the enhanced focusing of the chicane dipoles, where the dipole field is set by the injection/dump energy, but the edge focusing is determined by the energy of the accelerated beams. Both could be compensated by linear retuning of the standard bERLinPro optics. The bERLinPro project goal parameters, mainly the emittance of well below $1 \times 10^{-6} \pi$ mm mrad and the bunch length of 2 ps in the straight section, could be reached also with the MESA linac, without adjusting the emittance compensation scheme, the sextupole configuration or the chirp imprinted in the linac cavities, Fig. 8. Differences do

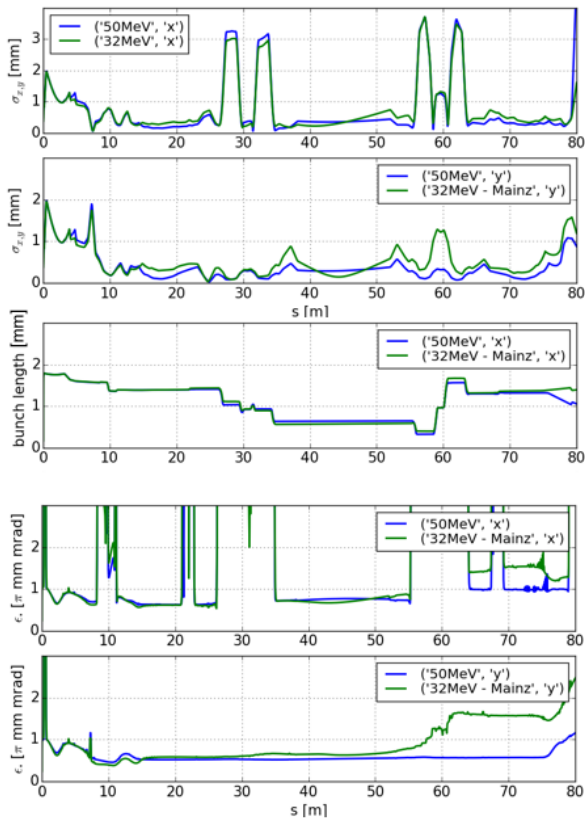


Figure 8: The optics for both linacs achieve the bERLinPro project goals in the straight section.

arise though, as the optics is now space charge dominated from cathode to dump, and micro bunching and coherent synchrotron radiation (CSR) effects dominate the emittance.

Micro bunching and CSR effects

Micro bunching structures can occur on the longitudinal current distribution. First, shot noise from the cathode laser

leads to density modulations in the particle distribution. In combination with space charge forces these density modulations are transferred to energy modulations, which, in combination with R56, turn into micro bunching structures or might also be diluted. The bunching factor is defined as the Fourier transform of the current distribution, and given by

$$b(\lambda) = \frac{1}{N_{ec}} \int I(z) e^{-\frac{i2\pi z}{\lambda}} dz; \quad (1)$$

Fig. 9 shows the longitudinal phase space for the bERLinPro optics (left) and the optics with the MESA linac (right) at the beginning of the straight section. The enhanced energy modulations in the MESA case are clearly visible. Fig. 10 shows the according bunching factor of both bunches. There is a 50 to 100 % increase in bunching between 30 and slightly above 100 μ m wavelengths for the MESA optics. To detect

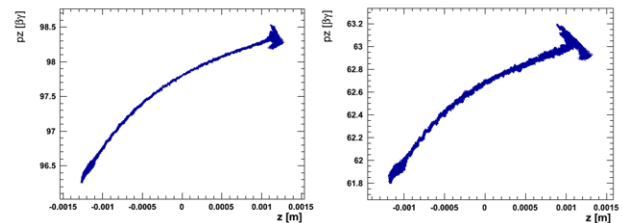


Figure 9: Longitudinal phase space at the beginning of the straight section. Left: bERLinPro optics. Right: optics with MESA linac. The enhanced energy modulation is clearly visible.

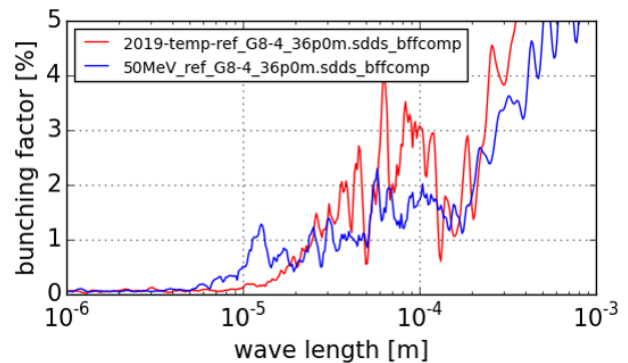


Figure 10: The bunching factor of the MESA bunch exceeds that of bERLinPro by 50 to 100 %.

these micro bunching structures and investigate to which extent they cause bunch degradation due to CSR radiation, intensive tracking simulations are necessary. The grid size for space charge calculations has to resolve the bunching wavelengths, and the number of tracked electrons has to be chosen accordingly. In the tracking code OPAL, [3], we use a grid of 2^{21} in different combinations, depending on the bunch form, and 2.4×10^6 particles. Using 64 cores on the HZB cluster, tracking 1 m through bERLinPro roughly only takes 30 min, due to the efficient parallelization of OPAL.

No enhancement of micro bunching due to CSR radiation could be observed in either case. But CSR effects do cause a loss of energy of 10 keV in both cases. They also deteriorate the emittance in both cases, although much stronger for the optics with the MESA linac. It should be noticed, that due to the enhanced grid size and the vast amount of particles, the emittance already increases by 15% for both optics, compared to the standard grid of 32^3 and 10^5 particles. The increase due to space charge, and due to the combination of space charge and CSR is listed in Table 1. The emittance

Table 1: Increase of the Horizontal Emittance after First Arc

E [MeV]	Emittance [π mm mrad]	
	space charge	space charge and CSR
50	0.778 (+18%)	0.837 (+6%)
30	1.420 (+101%)	2.050 (+44%)

blow up due to space charge exceeds that due to CSR by almost a factor of three. While for the bERLinPro case the emittance values stay within the project goals, at reduced energy, the horizontal emittance is doubled. This could not be seen in the standard tracking calculations with a decent number of grid cells and particles.

The longitudinal space charge impedance is a property of the vacuum chamber of the dipoles and reflects the frequency range, where matching frequencies in the current profile of the bunch could potentially be enhanced according to $V(\omega) = I(\omega) \cdot Z(\omega)$, with I, the Fourier transform of the current profile of the bunch, Z, the impedance, and V, the resulting frequency dependent voltage. Following the approach of Venturini, [8], who takes a 3D shot noise model into account for an analytic expression of the longitudinal space charge impedance, one can derive the space charge impedance for both optics, considering the different particle energies and different average radii of the bunches, as shown in Fig. 11.

The impedance is shifted towards shorter wavelengths for higher energies. For identical bunch radii, higher energy leads to a reduction of the amplitude of the impedance. For the average radii in the first arc of 0.5 mm in the 30 MeV MESA optics, compared to 0.3 mm in the 50 MeV bERLinPro optics, the amplitude of the impedance is similar. This agrees well with the result of the tracking studies. Fig. 12 shows the gain of the first arc, i.e. the ratio between the bunching at the end of the arc and the bunching at the beginning. We see the same signature as in the analytic formula. The wavelength of maximum increase of bunching is shifted towards shorter wavelength for higher energy and the amplitude for the lower energy but larger bunch radius is only slightly smaller. The independence of the gain of the initial particle distribution is shown in Fig. 13.

CONCLUSION

During the turn of the project bERLinPro many different adaption of the optics to changing hardware realizations had

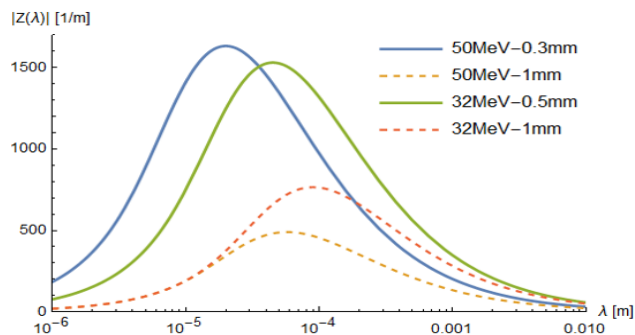


Figure 11: Longitudinal space charge impedance model for two energies and different radii.

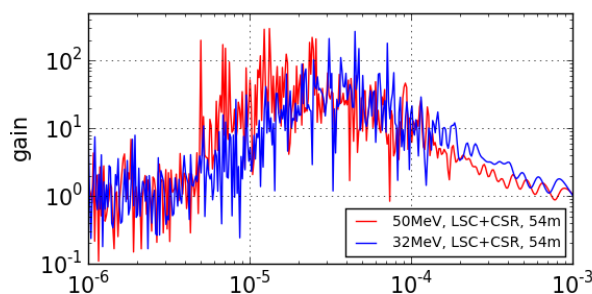


Figure 12: The gain as a function of the wavelength calculated by tracking follows the same dependencies on energy and beam radius as predicted by the analytical formula.

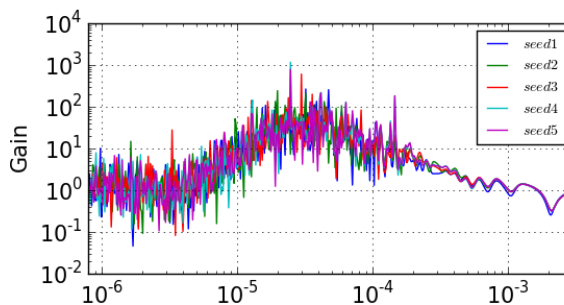


Figure 13: Gain in first arc calculated for 5 different seeds.

to be handled and different challenges had to be met. Examples were given for each of the three parts of the machine: the diagnostics line, the Banana and the recirculator. The measurement of the magnetic field in the accelerator hall led to the installation of corrector coils in the booster module. Ways to correct the trajectory in the diagnostics line and the Banana despite the lack of sufficient BPMs have to be developed. The sources of unwanted beam in the injector have been studied, and sources of halo leading to emittance dilution have been identified. In the recirculator it was found that the employment of the MESA linac module will prohibit to achieve the project goal of seeking an emittance of below $1 \times 10^{-6} \pi$ mm mrad in the straight section, due to space charge and CSR effects, that were of no concern with the higher energy foreseen for the bERLinPro linac.

REFERENCES

- [1] M. Abo-Bakr et al., “The Berlin Energy Recovery Linac Project bERLinPro – Status, Plans and Future Opportunities”, presented at ERL’19, Berlin, Germany, Sep. 2019, paper: MOCOXBS04, this conference.
- [2] B. Kuske, A. Adelman, “Commissioning of the bERLinPro Diagnostics Line using Machine Learning Techniques”, presented at ERL’19, Berlin, Germany, Sep. 2019, paper: WECOYBS05, this conference.
- [3] http://amas.web.psi.ch/docs/opal/opal_user_guide-2.0.0.pdf
- [4] B. Kuske, J. Rudolph, “Beam Positioning Concept and Tolerance Considerations for bERLinPro”, TUPRO038, in *Proc. IPAC’14*, Dresden, Germany, 2014. doi:10.18429/JACoW-IPAC2014-TUPRO038
- [5] B. Kuske, Ch. Metzger-Kraus, “Start-to-end Calculations and Trajectory Correction for bERLinPro”, in *Proc. IPAC’16*, Busan, Korea, 2016. doi:10.18429/JACoW-IPAC2016-THOBA03.
- [6] M. McAteer, “Dark current and halo tracking in ERLs”, presented at ERL’17, Geneva, Switzerland, Jun 2017, paper TH1-ACC002, unpublished.
- [7] W. Anders, K. Aulenbacher, F. Hug, A. Jankowiak, B. Kuske, A. Neumann, T. Stengler, C.P. Stoll, “Incorporation of a MESA Linac Modules into bERLinPro”, in *Proc. IPAC’19*, Melbourne, Australia, May 2019, pp. 1449–1452, doi:10.18429/JACoW-IPAC2019-TUPGW023
- [8] M. Venturini, “Models of longitudinal space - charge impedance for microbunching instability”, *Phys. Rev. ST Accel. Beams*, vol. 11, p. 034401 (2008). doi=10.1103/PhysRevSTAB.11.034401